AD-A129 912 LECTURES ON MATHEMATICAL COMBUSTION LECTURE 6 CELLULAR FLAMES..(U) CORNELL UNIV ITHACA NY DEPT OF THEORETICAL AND APPLIED MECHAN.. J D BUCKMASTER ET AL. JAN 83 1/1

UNCLASSIFIED TR-151 ARO-18243.22-MA DAAG29-81-K-0127 F/G 21/2 NL

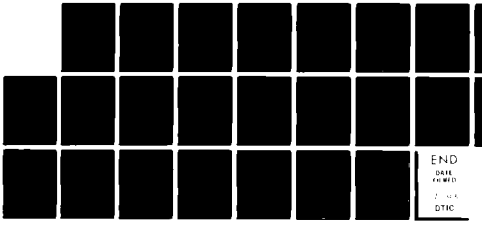

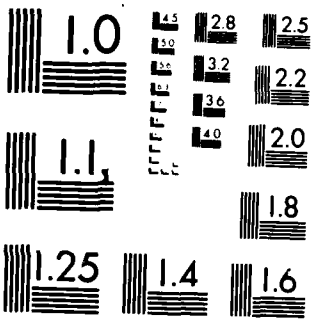

Cornell University

LECTURES ON MATHEMATICAL COMBUSTION

Lecture 6: Cellular Flames

Technical Report No. 151

J.D. Buckmaster & G.S.S. Ludford

January 1983

Theoretical and Applied Mechanics

Thurston Hall

Ithaca, New York

LECTURES ON MATHEMATICAL COMBUSTION

Lecture 6: Cellular Flames

Technical Report No. 151

J.D. Buckmaster & G.S.S. Ludford

January 1983

U.S. Army Research Office
Reserach Triangle Park, NC 27709

Contract No. DAAG29-81-K-0127

Cornell University
Ithaca, NY 14853

The view, opinions, and/or findings contained in this report are those of the authors and should not be construed as an official Department of the Army psosition, policy or decision, unless so designated by other authorized documents.

Contents

Lecture 6

CELLULAR FLAMES

We shall now examine the left stability boundary that was uncovered in lecture 5 in our discussion of NEFs (figure 5.3). The boundary is associated with instabilities leading to cellular flames, i.e. flames whose surfaces are broken up into distinct luminous regions (cells) separated by dark lines. Each line is a ridge of high curvature, convex towards the burnt gas. For a nominally flat flame these cells are very unsteady, growing and subdividing in a chaotic fashion; but curvature, for example, can make them stationary.

The most striking manifestation of cellular instability is the polyhedral flame, into which the conical flame on a Bunsen burner can suddenly transform. The conical surface splits into triangular cells forming a polyhedron; for a five-sided flame the appearance, from above, is much like that of the Chrysler emblem (figure 1). The dark wedges between the white triangular cells correspond to sharp ridges; the dark central region corresponds to a tip with strong curvature. Figure 2 gives a sketch of a five-sided flame, derived from a photograph in Smith & Pickering (1929). Polyhedral flames are often stationary, but can spin rapidly about the vertical, making several revolutions per second.

We shall discuss chaotic and stationary cellular flames, including polyhedral flames, in the framework of the weakly-nonlinear theory pioneered by Sivashinsky. The constant-density approximation will be used throughout, although perturbations of it will be admitted in two places.

1. Chaotic Cellular Structure.

The nonlinearity associated with the left stability boundary will be weakest in the neighborhood of

$$\bar{\ell} = -1, \quad k = 0,$$

a possible bifurcation point; accordingly we focus our attention there by taking

$$\bar{\ell} + 1 = O(\varepsilon), \; k = O(\sqrt{\varepsilon}), \; \alpha = O(\varepsilon^2), \tag{2}$$

where ε is a small positive parameter that will be found to represent the amplitude of the disturbance. The relative ordering of $\bar{\ell}+1$ and k is suggested by the parabolic shape of the stability boundary, while the order of α follows from the limiting form (5.49) of the dispersion relation (5.39) as $\varepsilon \to 0$. This determines the growth rate of the most important Fourier components (the unstable ones) of the disturbance when $\bar{\ell}+1$ is small. In terms of any scalar F that represents the disturbance field, the dispersion relation is equivalent to

$$F_t + 4F_{yyyy} - (1+\bar{\ell})F_{yy} = 0. \tag{3}$$

For $\bar{\ell}+1 < 0$, this equation predicts unbounded growth. Bifurcation (with weakly nonlinear description) is possible if nonlinear effects, not yet taken into account, limit this growth. We shall first give a heuristic argument to determine these effects and then substantiate the result by formal analysis. The argument consists in recognizing that equation (3) is actually a formula for the wave speed, and modifying it appropriately. In this connection, suppose that F determines the location of the flame sheet as

$$x = -t + \varepsilon F; \tag{4}$$

then the speed of the sheet is

$$W = 1 + \varepsilon W_1 + \ldots \text{ with } W_1 = -F_t, \tag{5}$$

and equation (3) becomes

$$W_1 = 4F_{yyyy} - (1+\bar{\ell})F_{yy}. \tag{6}$$

This formula determines the deviations of the flame speed from its adiabatic value of 1 due to the reaction-diffusion effects that are triggered by the distortion of the flame front.

Now, equation (5b) is mere kinematics, valid in a linear theory only. The exact relation between flame speed and displacement is

$$W = \frac{1-\varepsilon F_t}{\sqrt{1+\varepsilon^2 F_y^2}} = 1-\varepsilon F_t - \tfrac{1}{2}\varepsilon^2 F_y^2 + \ldots \tag{7}$$

and, for disturbances with wave-numbers of the magnitude (2b), the nonlinear terms $\frac{1}{2}\varepsilon^2 F_y^2$ is comparable to the linear term εF_t. This suggests that the nonlinear generalization

$$W_1 = -F_t - \tfrac{1}{2}\varepsilon F_y^2 \tag{8}$$

should be used in the formula (6) and, when ε is purged from the resulting equation by writing

$$\bar{\ell}+1 = -\varepsilon, \quad \eta = \sqrt{\varepsilon}y, \quad \tau = \varepsilon^2 t \tag{9}$$

(in accordance with the ordering (2)), we find

$$F_\tau + \tfrac{1}{2}F_\eta^2 + 4F_{\eta\eta\eta\eta} + F_{\eta\eta} = 0. \tag{10}$$

Note that this equation hold for $\bar{\ell} < -1$.

Substantiation of this result requires a systematic asymptotic development in which x is replaced by the coordinate

$$\eta = x + t - \varepsilon F(\eta,\tau) \tag{11}$$

in the governing equations (4.24,25); thus,

$$\partial/\partial x = \partial/\partial n,\ \partial/\partial y = -\varepsilon^{3/2}F_\eta\,\partial/\partial n+\varepsilon^{\frac{1}{2}}\partial/\partial\eta,\ \partial/\partial t = (1-\varepsilon^3F_\tau)\partial/\partial n+\varepsilon^2\partial/\partial\tau \qquad (12)$$

when y, t are replaced by η,τ. The normal derivative, required for the jump conditions (4.27-29), is

$$(1+\tfrac{1}{2}\varepsilon^3F_\eta^2)\partial/\partial n-\varepsilon^3F_\eta\,\partial/\partial\eta \qquad (13)$$

to sufficient accuracy. Perturbation expansions in ε are now introduced for T, h, and F, leading to a sequence of linear problems for the T- and h-coefficients as functions of n,η, and τ. These are to be solved under the requirements: $T_1 = T_2 = T_3 = \ldots = 0$ for $n > 0$; conditions as $n \to -\infty$ are undisturbed; and exponential growth as $n \to +\infty$ is disallowed. The problems are overdetermined, but only at the fourth (for T_3,h_3) is a solvability condition required, namely equation (10) for the leading term in F.

For two-dimensional disturbances of the flame sheet, the basic equation is

$$F_\tau + \tfrac{1}{2}(\nabla F)^2 + 4\nabla^4F + \nabla^2F = 0. \qquad (14)$$

Discussion for both one- and two-dimensional disturbances has been limited to numerical computations. The solutions obtained display chaotic variations in a cellular structure, resembling the behavior of actual flames. Figure 3 clearly shows the ridges that separate the individual cells.

2. Effect of Curvature.

Equation (10) is a balance of small terms; it may be modified to account for any additional physical process whose effect is also small. Hydrodynamic effects can be incorporated, for example, if the density change across the flame is appropriately small (because of small heat release), and this provides important insight into the role of Darrieus-Landau instability in actual flames. Equation (10) is replaced by

$$F_\tau + \tfrac{1}{2}F_\eta^2 + 4F_{\eta\eta\eta\eta} + F_{\eta\eta} + \gamma \int_{-\infty}^{\infty} \frac{F_\eta(\bar{\eta},\tau)}{\bar{\eta}-\eta}\, d\bar{\eta} = 0 \quad \text{with } \gamma = \frac{\sigma-1}{2\pi\varepsilon^{3/2}}\,, \tag{15}$$

the requirement on the heat release being $\gamma = O(1)$: the expansion ratio σ can only differ from 1 by $O(\varepsilon^{3/2})$. Numerical integration shows that the new (integral) term is destabilizing; an even finer structure is superimposed on the chaotic cellular pattern obtained without it. We shall not consider the topic further, since Sivashinsky (1983) has recently discussed it in detail. Instead, we shall examine a much simpler effect, that of curvature.

Consider a line source of mixture supporting a stationary cylindrical flame; the radial speed of the efflux is taken to be

$$u = R/r, \tag{16}$$

where R is an assignable constant. The corresponding solution of equations (4.24,25), the jump conditions (4.27-29), and the boundary conditions at the origin and infinity show that the flame is located at $r = R$ and that

$$T = \begin{cases} T_f + Y_f (r/R)^R \\ \\ T_f + Y_f \end{cases}, \quad h = \begin{cases} \ell Y_f r^R \ln(R/r)/R^{R-1} \\ \\ 0 \end{cases} \quad \text{for } r \lesseqgtr R. \tag{17}$$

Note that the speed (16) is 1 at the flame location, an unexpected result. Apparently the effect of flame curvature on its speed, normally significant, is here cancelled by the effect of flow divergence.

When R is $O(\varepsilon^{-2})$ the curvature is $O(\varepsilon^2)$, as for the disturbed plane flame described by equation (10). We would therefore expect such large flames, if disturbed to the same extent, to be described by a modification of that equation; the additional terms will be due to flow divergence and undisturbed curvature. The modified equation can be derived by formal

expansion, as was the original; but such an exercise, although reassuring, is hardly illuminating. We shall instead give a heuristic derivation that emphasizes the physics.

The general effect of large-scale (and therefore weak) stretch on flame speed was identified in section 4.5; we may write

$$W = 1 - (1+\bar{\ell})K + \ldots, \tag{18}$$

where K is the Karlovitz stretch (4.3). This effect is the origin of the second term on the right side of equation (6); the first, corresponding to what is normally a small correction to the result (18), must be retained when $\bar{\ell}$ is close to -1. In the present context, where flow divergence generates a stretch R^{-1} of order ε^2 in the undisturbed plane flame, equation (6) has to be replaced by

$$W_1 = 4F_{yyyy} + \varepsilon F_{yy} + R^{-1}. \tag{19}$$

Note that F still represents disturbance of a plane flame, so that the description is valid only up to $O(\varepsilon^{-\frac{1}{2}})$ values of y.

The kinematic expression (8) for the wave speed is also modified, because the flame sheet is moving in a non-uniform velocity field. We find

$$W_1 = -F_t - yF_y/R - F/R - y^2/\varepsilon R^2 - \tfrac{1}{2}\varepsilon F_y^2 \tag{20}$$

to sufficient accuracy, so that combination with the result (19) now yields

$$F_t + \frac{\varepsilon}{2}F_y^2 + 4F_{yyyy} + \varepsilon F_{yy} + F/R + yF_y/R = -y^2/\varepsilon R^2 - 1/R. \tag{21}$$

This has the stationary solution

$$F = F_0 \equiv -y^2/2\varepsilon R \tag{22}$$

corresponding to the undisturbed circular flame. Replacing F by $F+F_0$, so that F now represents disturbance of the circular flame sheet, and using the scaled variables (9) yield

$$F_\tau + \tfrac{1}{2}F_\eta^2 + 4F_{\eta\eta\eta\eta} + F_{\eta\eta} + \gamma F = 0 \text{ with } \gamma = 1/\varepsilon^2 R. \tag{23}$$

Comparison with equation (10) shows that the only new term is γF.

The linearized form of equation (23), with F set proportional to $\exp(\alpha t+iky)$, was considered in section 5.4. Figure 5.5 shows that curvature is a stabilizing influence, but that instability occurs for

$$\gamma < \gamma_c = 1/16, \tag{24}$$

corresponding to a supercritical bifurcation with wavenumber

$$k_c = \sqrt{\varepsilon/8}. \tag{25}$$

To show this we write

$$\gamma = \gamma_c - \delta^2, \quad F = \delta f, \quad \tau = \tilde{\tau}/\delta^2 \tag{26}$$

and expand f is a power series in δ. In the usual way, we find that the leading term is of the form

$$f_0 = A(\tilde{\tau})e^{ik_c y} + \bar{A}(\tilde{\tau})e^{-ik_c y}, \tag{27}$$

where

$$dA/d\tilde{\tau} = A - \bar{A}A^2/36 \tag{28}$$

if there is to be no secular term in the second perturbation of f. The equation describes the evolution in (slow) time $\tilde{\tau}$ of the amplitude from some initial value to the final value $|A| = 6$.

An examination of the first perturbation of f reveals that the crests of the final stationary solution, as viewed from the burnt gas, are sharper than the troughs. Moreover, the flame temperature is diminished at the crests (as for the cellular flames discussed in section 5.3), so that they are darker than the rest of the flame sheet. Sharp, dark crests are a universal feature of cellular flames as observed.

3. Flames Near a Stagnation Point.

Equation (23) is only one of a class of evolution equations that describe cellular flames in a variety of circumstances. An unusual example corresponds to a flame located in weak stagnation-point flow

$$\underset{\sim}{v} = \beta(-x,y) \quad \text{with } \beta = O(\varepsilon^2). \tag{29}$$

Two changes have been made in the notation of section 4.5: the x,y-axes have been rotated, so that the wall is now $x = 0$ and the undisburbed flame at $x = x_* > 0$ (cf. figure 4.3), to conform with notation already established in this lecture; and the strain rate is now β, since the ε used there has been conscripted as a small parameter here. As for the cylindrical flame, we shall be content with a heuristic derivation.

The undisturbed flame experiences a stretch β so that, if it is displaced by an amount εF, its speed is

$$W_1 = 4F_{yyyy} + \varepsilon F_{yy} + \beta \tag{30}$$

to sufficient accuracy (cf. equation (19)). The kinematic expression for the wave speed, corresponding to the result (20), is

$$W_1 = (\beta x_* - 1)/\varepsilon - F_t - \beta\, yF_y - \beta F - \tfrac{1}{2}\varepsilon\beta x_* F_y^2. \tag{31}$$

Equating these two expressions for W_1 gives a formula for x_*, namely

$$x_* = 1/\varepsilon^2\gamma + \varepsilon \text{ with } \gamma = \beta/\varepsilon^2, \tag{32}$$

and an evolution equation for F:

$$F_\tau + \tfrac{1}{2}F_\eta^2 + 4F_{\eta\eta\eta\eta} + F_{\eta\eta} + \gamma(\eta F)_\eta = 0. \tag{33}$$

Comparison with equation (10) shows that the only new term is $\gamma(\eta F)_\eta$.

The generalization

$$F_\tau + \tfrac{1}{2}(\nabla F)^2 + 4\nabla^4 F + \nabla^2 F + \gamma(\eta F)_\eta = 0 \tag{34}$$

accounts for disturbances that vary in the z-direction also. If we now consider disturbances independent of η, this equation reduces to the earlier one (23) with η replaced by $\zeta = \sqrt{\varepsilon}z$. Setting F proportional to $\exp(\alpha t+ikz)$ and linearizing therefore leads to the dispersion relation (5.49) and hence to figure 5.5. The bifurcation analysis starting with the transformation (26) is applicable, so that for values of γ slightly smaller than $1/16$ there will be a stationary structure characterized by dark ridges pointing towards the burnt gas.

This phenomenon has apparently been known for many years. For upward propagation through sufficiently lean hydrogen-air mixtures in a standard flammability tube, the flame cap is divided into a number of bright strips or ribbons, separated by dark lines (figure 4); it seems probable that this is the axisymmetric analog of the nominally plane flame considered here. The straining flow is generated by the gravity-induced convection of the light burnt gas behind the flame (see, for example, Buckmaster & Mikoalitis 1982).

A different type of disturbance (which can be combined with the previous one without, however, adding to the discussion) corresponds to

$$F = a(\tau)\exp(ike^{-\gamma\tau}). \tag{35}$$

Substitution into the linearized version of the evolution equation (33) gives

$$dA/d\tau = A(k^2 e^{-2\gamma\tau} - 4k^4 e^{-4\gamma\tau} - \gamma), \qquad (36)$$

which has the solution

$$A = A_0 \exp[(1-e^{-2\gamma\tau})k^2/2\gamma + (e^{-4\gamma\tau}-1)k^4 - \gamma\tau]. \qquad (37)$$

Figure 5 shows that any disturbance eventually has a decreasing amplitude, although for a time the amplitude increases if γ is less than 1/16. In the limit $\tau \to \infty$, the solution (37) tends to zero. We conclude that the flame is stable to this type of disturbance.

The chaotic cellular instability found experimentally for weak straining suggests that all disturbances should grow. Moreover, in the limit $\gamma \to 0$ the theoretical results in lecture 5 predict instability for all (small) wavenumbers. These facts are at variance with the conclusion above, which prompted Sivashinsky, Law & Joulin (1982) to provide the following explanation.

If the nonlinear term is retained in equation (33), harmonics are continually generated and these may grow during part of their lifetime, providing a mechanism for sustaining the overall growth of the disturbance into instability. Numerical computations confirm this notion and suggests that the necessary values of γ are significantly smaller than 1/16. There may be implications for the hydrogen flame of figure 4. Away from the nose the rate of strain will be diminished, and may be small enough in the skirt to permit instabilities in the direction of the flow. That is, the ribbon instability may become a cellular instability. Interestingly enough, the tails of the ribbons are often seen to break up into small balls of flame (figure 4).

4. Polyhedral Flames.

In the 90 years since Smithells first observed these flames, they have become established as a familiar laboratory curiosity. They are associated with tube burners, but analogs can be created with different geometries: Markstein (1964, p. 81) designed a slot burner on which he observed a cellular flame behaving essentially like an unwrapped (linear) polyhedral flame. In particular, the cells could be made to travel rapidly from one end of the slot to the other, just as the polyhedral flame can be made to spin. Markstein's photographs of the flame showed that the traveling corrugations are saw-toothed in shape (figure 6).

It is the propagation that distinguishes polyhedral flames from other types of cellular instability, so that will be the focus of our discussion. Since the left stability boundary is not associated in any obvious way with propagating disturbances (unlike the right stability boundary), the challenge is to uncover a mechanism for such behavior.

One of the difficulties with polyhedral flames is that the undisturbed flame is conical, i.e. non-planar. Following Buckmaster (1983), we shall overcome this obstacle by adopting a nominally planar model. Consider the portion AB of the burner flame that is located near the rim (figure 7a). The flame speed varies from a small value (perhaps zero) at A, to a value comparable to the adiabatic flame speed at B. This portion is modeled by a plane flame with some intermediate speed and standoff distance (figure 7b). Perturbations of the planar configuration are permitted in the y-direction, which is perpendicular to the page and parallel to the rim. Corrugations that arise in this way are associated with the corrugations along the entire length of the nominally concial-shaped flame whose base is being modeled.

In the context of the weakly nonlinear theory, perturbations are governed by equation (10), provided a term is added to account for the presence of the rim. The rim is a heat sink that anchors the flame in a simple fashion: an increase (decrease) in the standoff distance reduces (increases) the heat loss to the rim, thereby increasing (decreasing) the flame speed, a restorative mechanism. If F is now the perturbation of the standoff distance, this effect can be represented by the modification

$$W_1 = 4F_{yyyy} - (1+\bar{\ell})F_{yy} + qF \tag{38}$$

of the equation (6). Here q is a positive constant of order ε^2, and the factor $-(1+\bar{\ell})$ has been restored (since the parameter ε, which was earlier equated to it, will be given a different definition). From the kinematic result (8) we now see that the governing equation is

$$F_t + \tfrac{1}{2}F_y^2 + 4F_{yyyy} - (1+\bar{\ell})F_{yy} + qF = 0, \tag{39}$$

a result identical to the curvature equation (23) when the scaling (9) is undone and R^{-1} replaced by q.

The linearized form of this equation was considered in section 2, but we shall interpret the analysis differently. Rather than fixing $\bar{\ell}$ and determining the range of unstable wavenumbers for each q (there R^{-1}), we shall fix q and determine the range of unstable wavenumbers for each $\bar{\ell}$. Thus, with F proportional to $\exp(\alpha t+iky)$, the stability boundary $\alpha = 0$ is seen to be the curve

$$4k^4 + (1+\bar{\ell})k^2+q = 0 \tag{40}$$

shown in figure 8.

Not all values of k are admissible, however, because an integer number of wavelengths must fit around the burner rim. The length L of

the circumference provides the definition of the small parameter ε, namely

$$\varepsilon = 4\pi^2/L^2, \tag{41}$$

and then the restriction is

$$k = k_N \text{ with } k_N = N\sqrt{\varepsilon}\ , \ N = 1,2,3,... \tag{42}$$

The positions of the corresponding points on the neutral curve depend on the value of q; in drawing figure 8 we took $q = 117\varepsilon^2$. The corresponding values of $\bar{\ell}$ then lie in the order $\bar{\ell}_2,\bar{\ell}_3,\bar{\ell}_4,\bar{\ell}_5,\bar{\ell}_1,\bar{\ell}_6,\bar{\ell}_7,...$. For larger values of q there are more points on the lower branch of the curve: in general, for $q > 4M^4\varepsilon^2$ there are M.

Those points for which the (reduced) Lewis number of the mixture is less than $\bar{\ell}_N$ correspond to unstable modes. Thus, each $\bar{\ell}_N$ determines a supercritical bifurcation corresponding to a stationary N-sided polyhedral flame. Such unimodal bifurcations are essentially the same as those considered earlier in the context of flame curvature.

Both $\bar{\ell}$ and q can be varied in an experiment by changing the mixture strength and flow rate. We have seen that changes in q will move the points corresponding to k_N along the neutral curve, altering the stability characteristics of the flame. Changes in $\bar{\ell}$ will do so too. For certain choices of q, two bifurcation branches merge, i.e. $\ell_M = \ell_N$ for some M,N. The solution on such a merged branch corresponds to a spinning polyhedral flame, provided $M = 2N$.

The most satisfactory case, from a mathematical point of view, is $M = 2$, $N = 1$, (i.e. $q = 16\varepsilon^2$), for then the merged branch is the rightmost one and presumably is accessible as the first manifestation of instability. However one- or two-sided polyhedra do not fit comfortably on a circle, so that is not a physically satisfying choice. The objection does not apply

to the choice $M = 6$, $N = 3$ (i.e. $q = 1296\varepsilon^2$), but then the two branches originating at $\bar{\ell}_4$ and $\bar{\ell}_5$ lie to the right of the merged branch, and our elementary analysis can provide no evidence that the latter is accessible. Buckmaster does not resolve this difficulty but, instead, argues that the favorable comparison of the merged-branch solution with the physical flame is good evidence of accessibility.

To ensure that k_N and k_{2N} give the same $\bar{\ell}$, we must take

$$q = 16N^4\varepsilon^2, \tag{43}$$

and then

$$\bar{\ell}_N = \bar{\ell}_{2N} = -1-20N^2\varepsilon. \tag{44}$$

To determine the solution on the merged branch, we perturb q and $\bar{\ell}$ away from the values (43,44) by $O(\delta^2)$, where δ is a small perturbation parameter. At the same time we write

$$F = \delta f, \quad \tilde{t} = \tilde{t}/\delta \tag{45}$$

and expand f in a power series in δ. The leading term is found to be of the form

$$f_0 = A(\tilde{t})e^{ik_N y} + \bar{A}(\tilde{t})e^{-ik_N y} + B(\tilde{t})e^{ik_{2N} y} + \bar{B}(\tilde{t})e^{-ik_{2N} y}, \tag{46}$$

where

$$\partial A/\partial\tilde{t} = -2k_N^2\bar{A}B, \quad \partial B/\partial\tilde{t} = \tfrac{1}{2}k_N^2A^2 \tag{47}$$

if there is to be no secular term in the perturbation of f. Partial derivatives are used because A and B also depend on the slow time $\delta^2 t$; evolution on this scale determines the ultimate amplitude of the spinning flame, but we shall not pursue the matter here.

Equations (47) have solutions corresponding to

$$f_0 = A_0[\sqrt{3}\sin(\omega\tilde{t}+\phi\pm k_N y)-\cos 2(\omega\tilde{t}+\phi\pm k_N y)] \text{ with } \omega = k_N^2 A_0; \tag{48}$$

here A_0 and ϕ are real and constant on the $\tilde{t}$-scale. These are waves traveling in the negative/positive y-direction with an amplitude-dependent phase speed $k_N A_0$. The shape of the wave resembles the sawtooth profile in figure 6, and Buckmaster has argued that the propagation speed is consistent with the rapid rotations seen in experiments.

5. Other Cellular Flames.

So far we have been concerned with the evolution of the linear instabilities associated with values of $\bar{\ell}$ slightly less than -1. Various additional effects were incorporated into the basic nonlinear theory, and others could have been (Sivashinsky 1983). Our final remarks are concerned with values of $\bar{\ell}$ slightly greater than -1, where the linear stability of the flame can be destroyed by hydrodynamic effects.

The weakly nonlinear description is now

$$F_\tau + \tfrac{1}{2}F_\eta^2 + 4F_{\eta\eta\eta\eta} - F_{\eta\eta} + \gamma \oint_{-\infty}^{\infty} \frac{F_\eta(\bar{\eta},\tau)}{\bar{\eta}-\eta}\, d\bar{\eta} = 0 \quad \text{with} \quad \gamma = \frac{\sigma-1}{2\pi\varepsilon^{3/2}}. \tag{49}$$

Comparison with equation (15) reveals that the sign of $F_{\eta\eta}$ has been changed, because now the definition

$$\varepsilon = 1 + \bar{\ell} \tag{50}$$

is needed to obtain a positive parameter; η and τ still have the definitions (9b,c). Without the integral term, $F \to 0$ as $\tau \to \infty$ whatever the initial conditions are, corresponding to linear stability; as before, the hydrodynamic effects (represented by the integral) are destabilizing. Michelson and Sivashinsky's computations show that a progressive wave, consisting of stationary cells, eventually forms

provided the flame is not too large. For large flames, the chaotic cellular structure first found in section 1 reasserts itself.

The shape of this progressive wave satisfies a much simpler equation in the limit $\gamma \to 0$, i.e. for significantly larger departures of $\bar{\ell}$ from -1 than of σ from 1. Evolution is then on the scales $\gamma\eta$, $\gamma^2\tau$ rather than η,τ, so that the fourth derivative drops out. If a progressive wave is sought by setting $F_\tau = -V$, and $F_{\eta\eta}$ is neglected (a valid step where the curvature is not large), the result is

$$\tfrac{1}{2}F_\eta^2 + \gamma \int_{-\infty}^{\infty} \left(\frac{1}{\bar{\eta}-\eta} - \frac{1}{\bar{\eta}}\right) F_\eta(\bar{\eta})\,d\bar{\eta} = 0 \quad \text{with} \quad V = \gamma \int_{-\infty}^{\infty} \frac{F_{0\eta}(\bar{\eta})}{\bar{\eta}}\,d\bar{\eta}, \tag{51}$$

a nonlinear integral equation for the slope F_η.

The rough solution found by Sivashinsky was not very satisfactory and so McConnaughey, Ludford & Sivashinsky (1983) recently integrated the equation more accurately. A continuous periodic solution is shown in figure 9; the solution for any other period can be obtained from it by scaling η without changing V (there is no preferred wavelength in the linear theory). At the cusps, F_η has a logarithmic singularity, which makes the structure of the combustion field quite different from that of a Bunsen flame near its tip, for example. (Of course the singularity will be smoothed out by the neglected term $F_{\eta\eta}$, as Michelson and Sivashinsky's computations show.)

Of particular interest is the value

$$V = 1.4\gamma^2$$

obtained by McConnaughey, Ludford, and Sivashinsky. For an expansion ratio of $\sigma = 5$, this leads to a flame speed that is 1.6 times the plane adiabatic value, a result in surprisingly good agreement with measured

values (which range between 1.5 and 2). The theory, which assumes $\sigma - 1$ to be small, is not valid for such large expansion ratios, but nevertheless makes an accurate prediction. This type of success is one of the hallmarks of a great theory.

References

1. Buckmaster, J. (1983). Polyhedral flames--an exercise in biomodal bifurcation analysis. SIAM Journal of Applied Mathematics (in press).

2. Buckmaster, J. & Mikolaitis, D. (1982). A flammability-limit model for upward propagation through lean methand/air mixtures in a standard flammability tube. Combustion and Flame, 45, 109-19.

3. Markstein, G.H. (1964). Nonsteady Flame Propagation. AGARDograph No. 75. New York: MacMillan.

4. McConnaughey, H.V., Ludford, G.S.S., & Sivashinsky, G.I. (1983). A calculation of wrinkled flames. (Submitted for publication.)

5. Sivashinsky, G.I. (1983). Instabilities, pattern formation, and turbulence in flames. Annual Review of Fluid Mechanics (in press).

6. Sivashinsky, G.I., Law, C.K., & Joulin, G. (1982). On stability of premixed flames in stagnation-point flow. Combustion Science and Technology (in press).

7. Smith, F.A. & Pickering, S.F. (1929). Bunsen flames of unusual structure. U.S. Bureau of Standards Journal of Research, 3, 65-74.

Figure Captions

6.1 Chrysler emblem.

6.2 Five-sided polyhedral flame.

6.3 Numerical calculation of cellular flames. (Courtesy G.I. Sivashinsky.)

6.4 Flame in a standard flammability tube.

6.5 Curve in $k^2 e^{-2\gamma t}$, γ-plane determining sign of right side of equation (36).

6.6 Analog of spinning polyhedral flame for slot burner.

6.7 (a) Behavior of tube flame near rim of burner.
(b) Plane model of (a) used to describe polyhedral flames.

6.8 Linear stability regions for polyhedral flames, with admissible values of k .

6.9 Stationary wrinkling of an otherwise stable plane flame due to hydrodynamic disturbances; possible outcome of Darrieus-Landau instability.

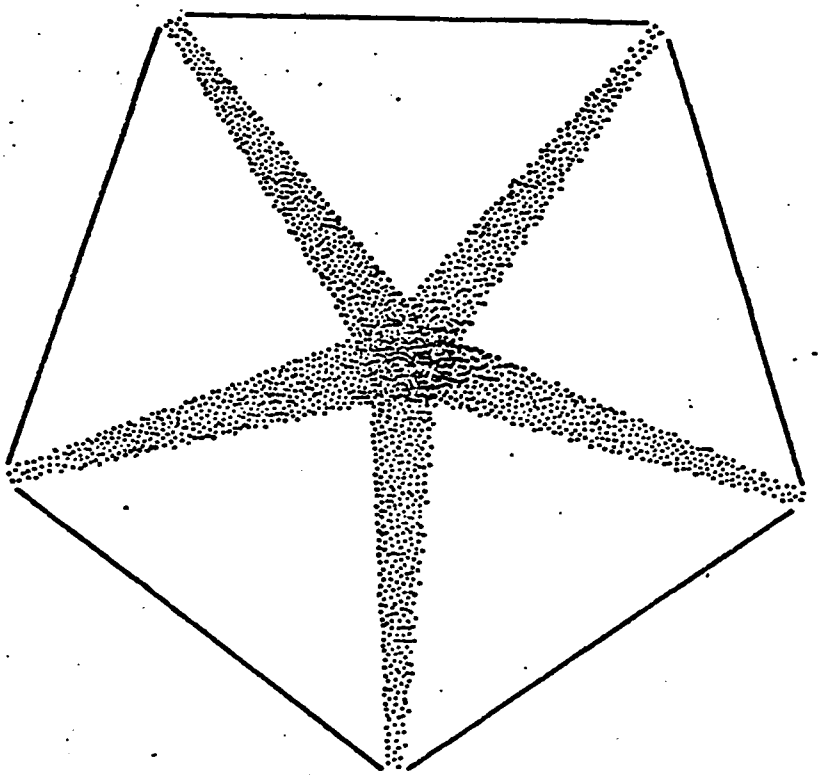

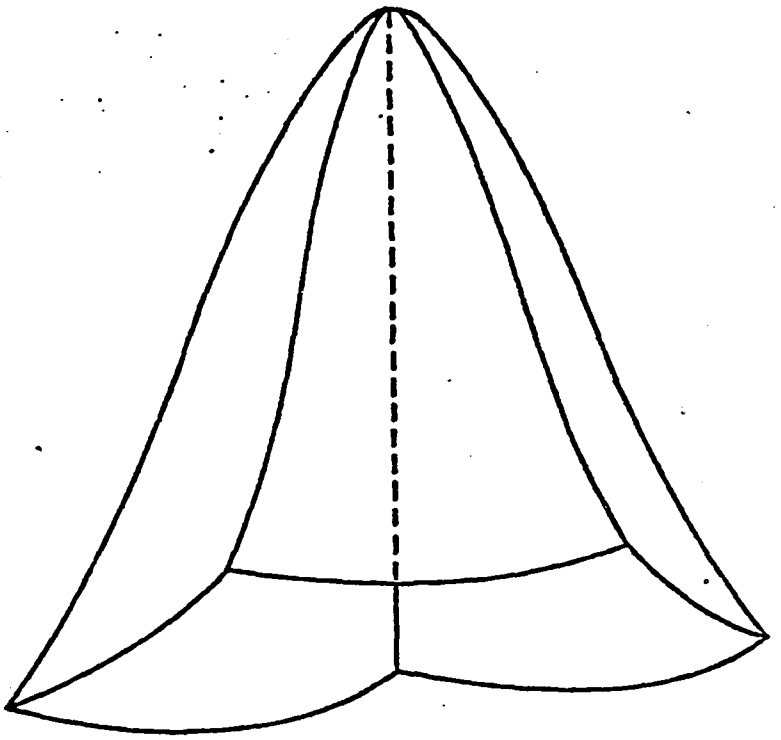

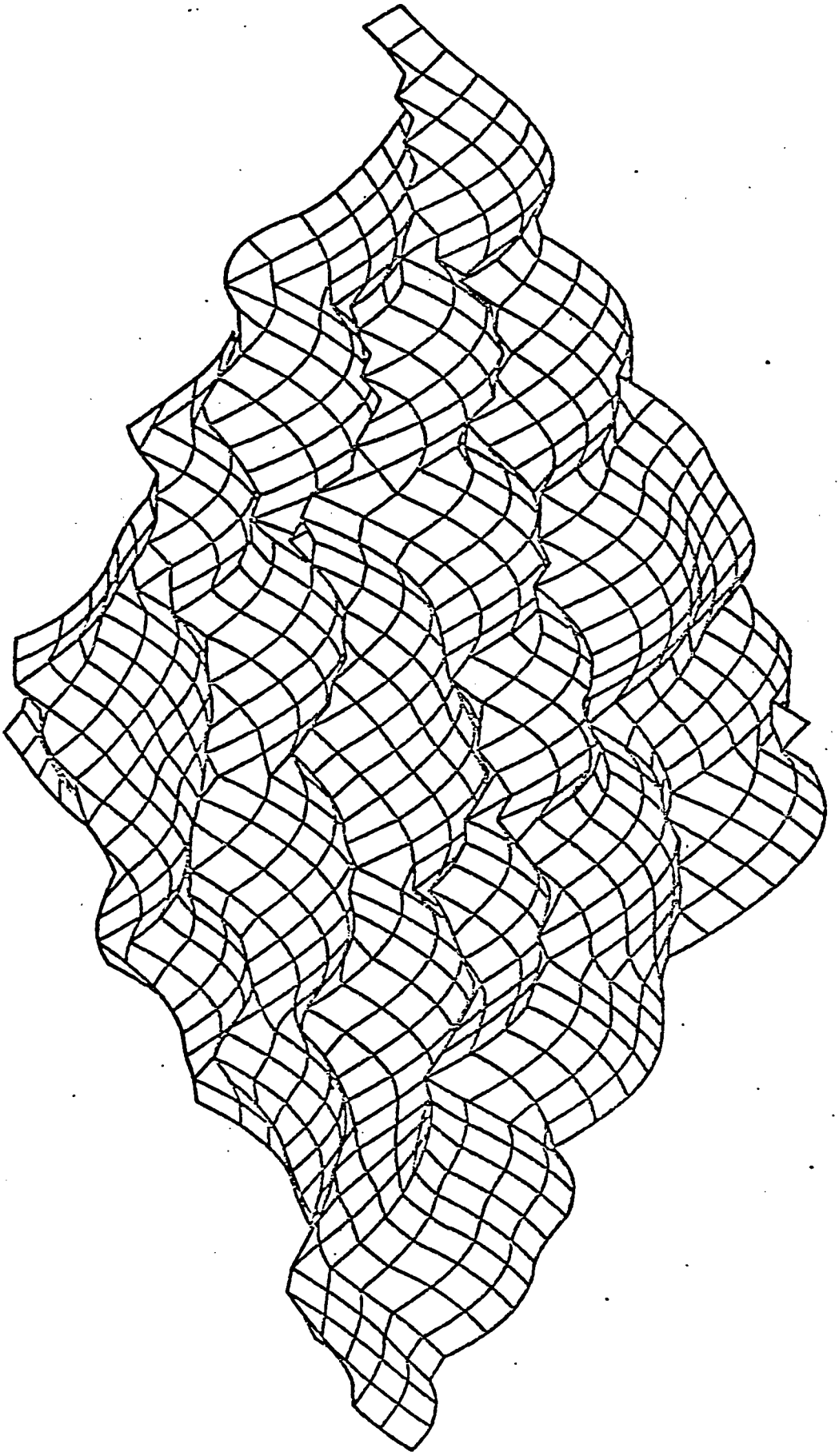

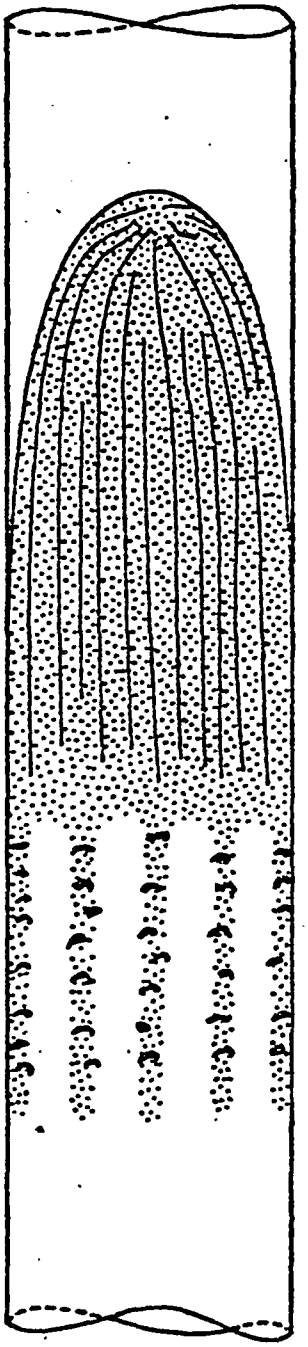

6.4

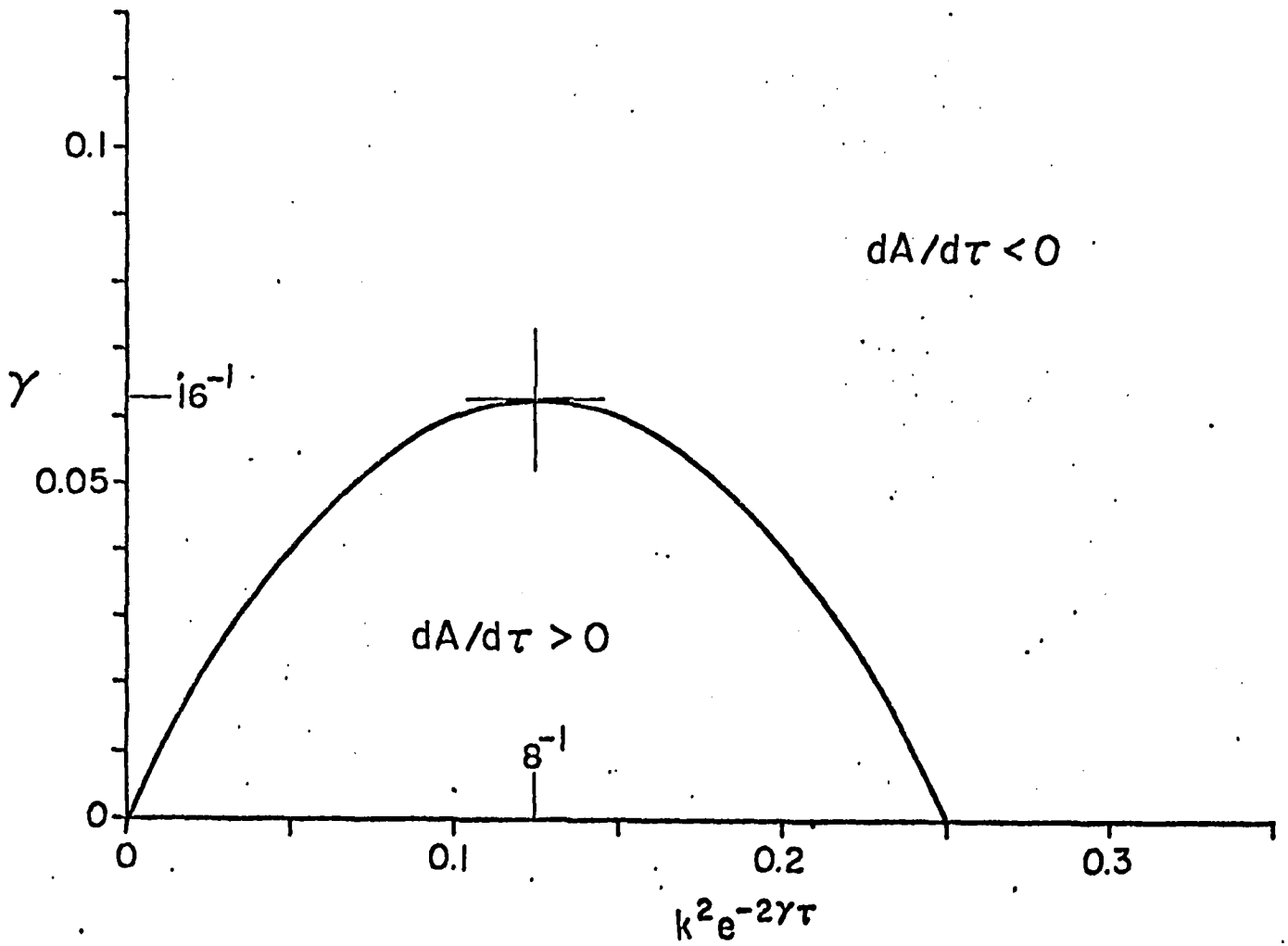
0.1
γ
16⁻¹
0.05
0
dA/dτ < 0
dA/dτ > 0
8⁻¹
0
0.1
0.2
0.3
k²e⁻²γτ

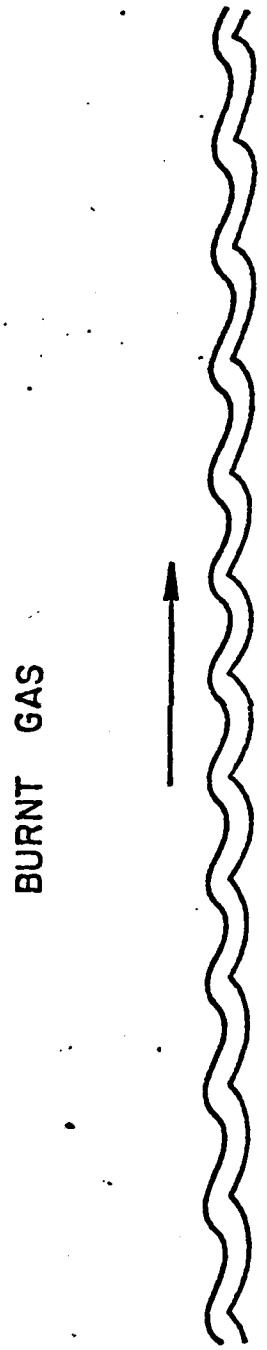
BURNT GAS
FRESH GAS

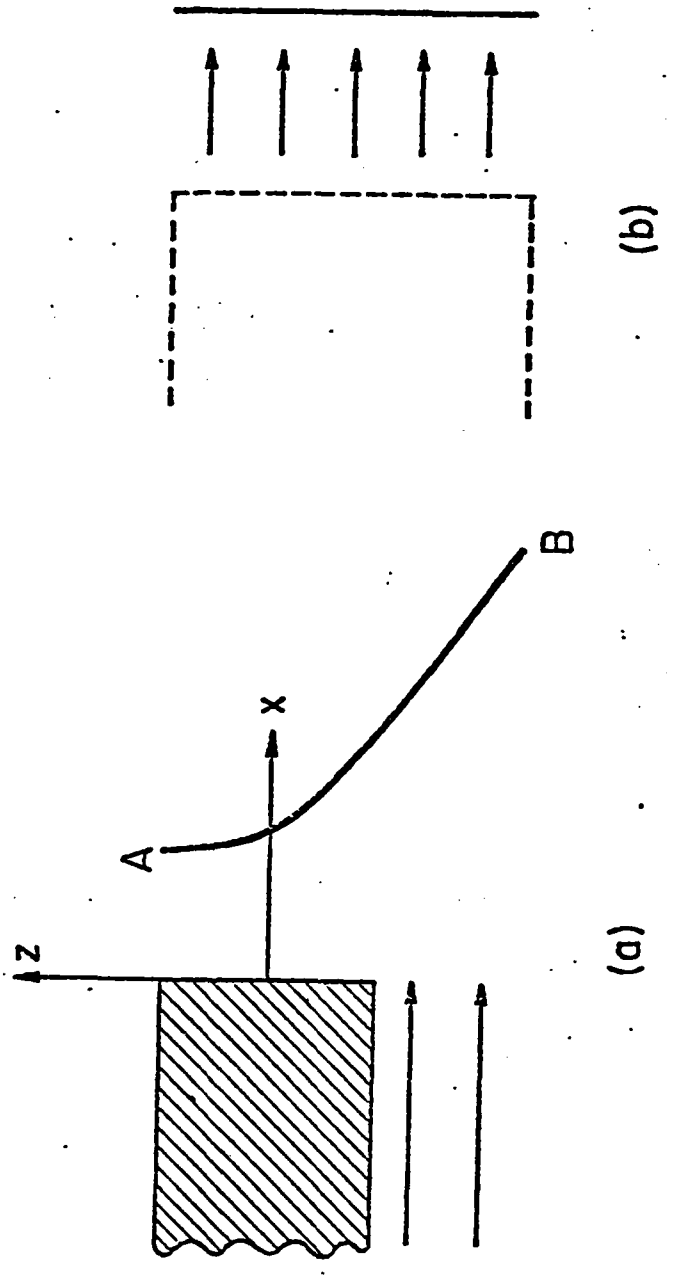

6.7

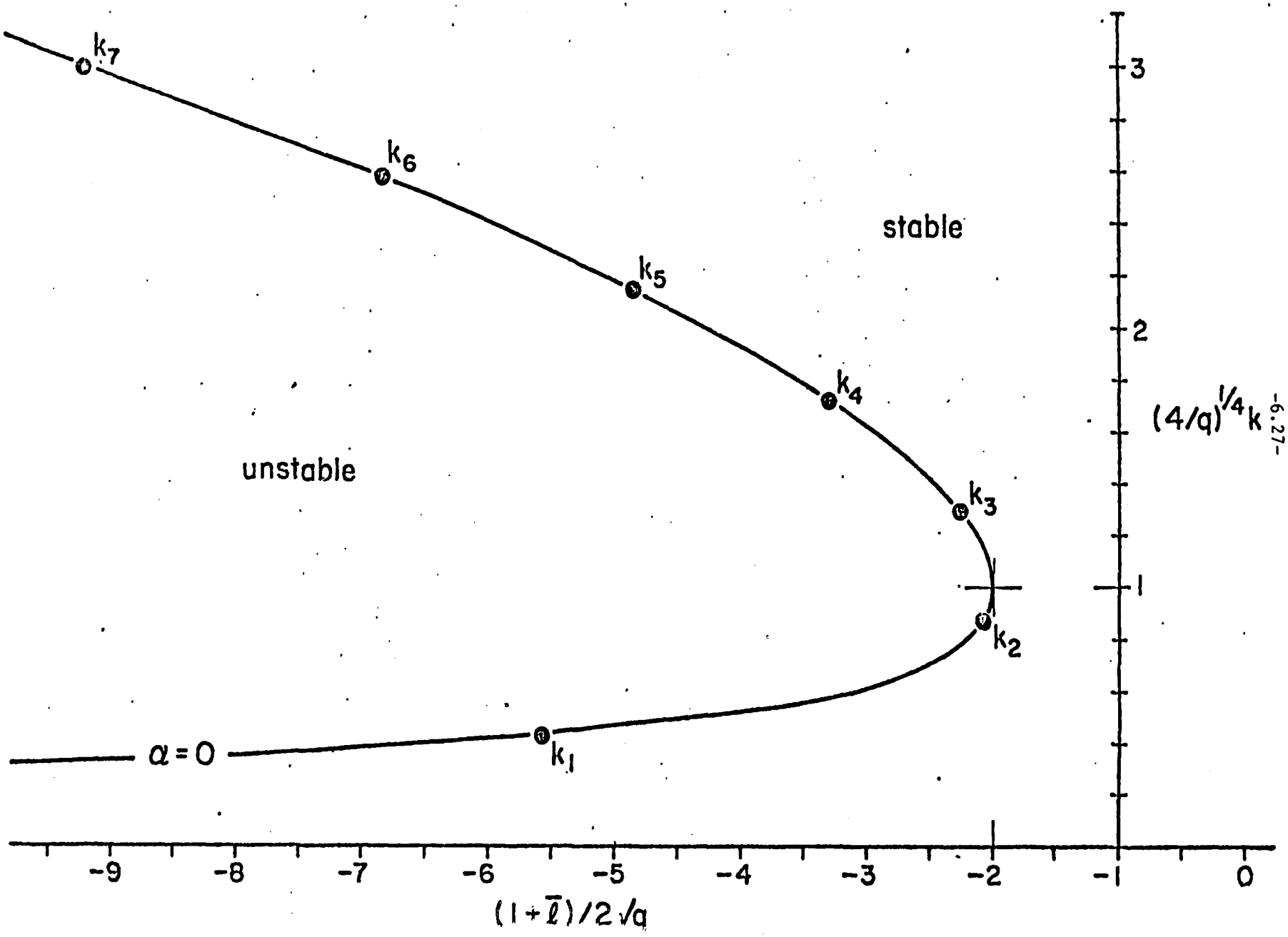
k_7
k_6
k_5
k_4
k_3
k_2
k_1
stable
unstable
$\alpha = 0$
-9
-8
-7
-6
-5
-4
-3
-2
-1
0
1
2
3
$(1+\bar{\ell})/2\sqrt{a}$
$(4/a)^{1/4} k$

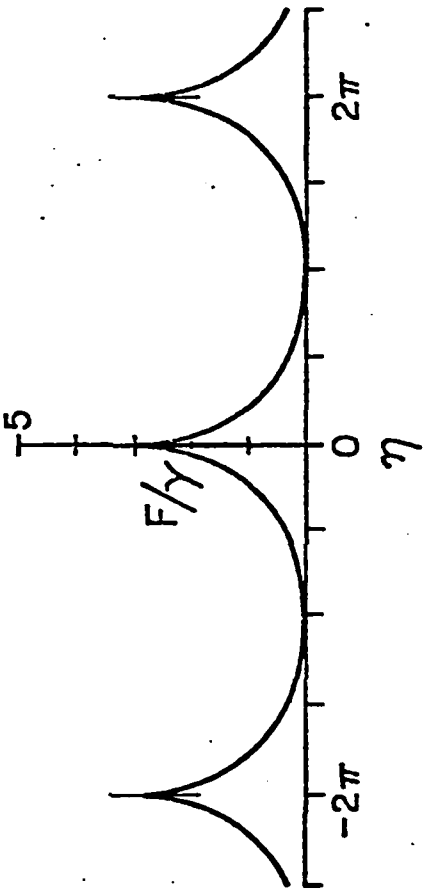

6.9

SECURITY CLASSIFICATION OF THIS PAGE (When Data Entered)

REPORT DOCUMENTATION PAGE		READ INSTRUCTIONS BEFORE COMPLETING FORM
1. REPORT NUMBER 151	2. GOVT ACCESSION NO. AD A129912	3. RECIPIENT'S CATALOG NUMBER
4. TITLE (and Subtitle) LECTURES ON MATHEMATICAL COMBUSTION Lecture 6: Cellular Flames		5. TYPE OF REPORT & PERIOD COVERED Interim Technical Report 6. PERFORMING ORG. REPORT NUMBER
7. AUTHOR(s) J.D. Buckmaster & G.S.S. Ludford		8. CONTRACT OR GRANT NUMBER(s) DAAG29-81-K-0127
9. PERFORMING ORGANIZATION NAME AND ADDRESS		10. PROGRAM ELEMENT, PROJECT, TASK AREA & WORK UNIT NUMBERS P-18243-M
11. CONTROLLING OFFICE NAME AND ADDRESS U. S. Army Research Office Post Office Box 12211 Research Triangle Park, NC 27709		12. REPORT DATE January 1983 13. NUMBER OF PAGES 28
14. MONITORING AGENCY NAME & ADDRESS(if different from Controlling Office)		15. SECURITY CLASS. (of this report) Unclassified 15a. DECLASSIFICATION/DOWNGRADING SCHEDULE

16. DISTRIBUTION STATEMENT (of this Report)

Approved for public release; distribution unlimited.

17. DISTRIBUTION STATEMENT (of the abstract entered in Block 20, if different from Report)

NA

18. SUPPLEMENTARY NOTES

THE VIEW, OPINIONS AND/OR FINDINGS CONTAINED IN THIS REPORT ARE THOSE OF THE AUTHOR(S) AND SHOULD NOT BE CONSTRUED AS AN OFFICIAL DEPARTMENT OF THE ARMY POSITION, POLICY, OR DECISION, UNLESS SO DESIGNATED BY OTHER DOCUMENTATION.

19. KEY WORDS (Continue on reverse side if necessary and identify by block number)

Chaotic and stationary cellular flames, stationary and spinning polyhedral flames, hydrodynamics destabilization, curvature effect, stagnation-point flow, flame ribbons.

20. ABSTRACT (Continue on reverse side if necessary and identify by block number)

We shall now examine the left stability boundary that was uncovered in lecture 5 in our discussion of NEFs (figure 5.3). The boundary is associated with instabilities leading to cellular flames, i.e. flames whose surfaces are broken up into distinct luminous regions (cells) separated by dark lines. Each line is a ridge of high curvature, convex towards the burnt gas. For a nominally flat flame these cells are very unsteady, growing and subdividing in a chaotic fashion; but curvature, for example, can make them stationary.

DD FORM 1 JAN 73 1473 EDITION OF 1 NOV 65 IS OBSOLETE

SECURITY CLASSIFICATION OF THIS PAGE (When Data Entered)

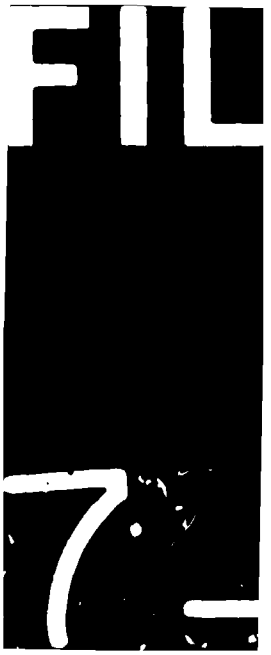
FIL